RSC Advances

ROYAL SOCIETY OF CHEMISTRY

www.rsc.org/advances

Journal Name

ARTICLE

Fabrication of PVDF membranes entrapped with oleic acid modified TiO_2 and selective adsorption toward bovine hemoglobin

Received 00th January 20xx,
Accepted 00th January 20xx

DOI: 10.1039/x0xx00000x

www.rsc.org/

Jianghua Zhang,[a] Shiguang Guo,[a] Yu Zhang,[b] Xia Zhang,[a*]Yufeng Liu, [b*] Junli Xu,[a] Yide Han[a] and Yan Xu[a]

An active protein adsorption membrane composed of poly(vinylidenedifluoride) (PVDF) and TiO_2 nanoparticles, which surface modified by oleic acid (OA) molecule has been fabricated. The hybrid membranes were obtained using an induc phase inversion method by blending the PVDF casting solution and OA-modified TiO_2 nanoparticles. The TiO_2 nanoparticles in anatase phase with average size ranged from 10 to 50 nm were entrapped into the pores and deposited the surface of PVDF films. Furthermore, the presence of TiO_2 nanoparticles affected the formation process of PVDF films and resulted in the variation of the pore structure of PVDF films. The adsorption performances of these PVDF hybrid membranes were measured using bovine hemoglobin (BHb) and bovine serum albumin (BSA) as target substances, and the effects of adsorption conditions were systematically studied to determine the optimum conditions. The adsorption results showed that the hybrid membranes had significant enhanced adsorption activity toward BHb and BSA in comparison with pure PVDF, and there was a positive relationship between adsorption capacity of proteins and the loading amounts of TiO_2. However, The OA-modification enhanced the BHb adsorption and meanwhile depressed the BSA adsorption. Interestingly the adsorption capacity of BHb on hybrid membranes was as 3-4 times as that of BSA. Using the mixed protein solution as adsorption object, the SDS-PAGE analysis demonstrated that BHb can be selectively adsorbed on the hybrid membranes. This work showed a prospect application of these hybrid membranes in the selective adsorption and separation of BHb.

Introduction

Separation and purification of protein from biological mixtures have played more and more important role in various areas, such as agro-food, biomedicine and bio-filtration applications. A series of techniques, including electrophoresis, precipitation, ultrafiltration, centrifugation and adsorption have been explored to separate proteins mixtures [1-4]. Among these methods, adsorption process has been widely used due to its lower cost, time-efficiency and ease in processing [3,4]. Different kinds of materials, inorganic or organic compounds were employed as adsorbents in the proteins adsorption. However, the protein adsorption at solid/liquid phase is complicated; the driven forces may arise from electrostatic, hydrophobic or chemical forces among the side chains of the protein and the reactive groups at surface of adsorbents [5,6]. Many factors can affect the adsorption efficiency, for example, interface properties, hydrodynamic conditions and solution environment including ionic strength, pH conditions and surface potential and so on. Sometimes the contradictory results may be obtained even using the same proteins as target substance. Therefore, in-depth understanding of the protein adsorption process is essential and useful in controlling the interaction between proteins and interfaces well so as to achieve higher adsorption efficiency and selectivity [7-9].

Nano-adsorbents have been attracting more attentions because of their large surface area to volume ratios and high interface activity. Some inorganic nano-materials, such as silica [10], aluminum oxide [9,11], ferroferric oxide [7,12] and carbon nanotube[13] present good adsorption-desorption activity for metal ions and bio-molecules. Titanium dioxide (TiO_2) presented good adsorption activity in the removal of inorganic ions, such as Pb(II), Cu(II), Ag(I) and Hg(II) [14-18], which was also applied in the protein adsorption for its excellent biocompatibility, non-toxicity and non-inflammatory properties [5,19-21]. For example, Kopac *et al.* [5] studied the BSA adsorption on TiO_2 nanoparticles, and determined the optimum adsorption conditions. Giacomelli *et al.* [21] investigated the BSA adsorption at the TiO_2-NaCl interface as a function of pH and electrolyte concentration. It was

[a] Department of Chemistry, College of Sciences, Northeastern University, Shenyang 110819, China.E-mail: xzhang@mail.neu.edu.cn; Tel: +86 24 83684533; Fax: +86 24 83684533
[b] College of Pharmacy, Liaoning University, Shenyang, 110036, China. E mail:liuyufeng@bimu.edu.cn: Tel: +86 2462202469

reported that the adsorption process was fast and reached its maximum at around the isoelectric point of BSA, and the BSA adsorption was insensitive toward electrolyte concentrations.

Surface modification with some active anchors, such as $–NH_2$, -SH, -COOH, $-SO_2OH$ and $–PO(OH)_2$ groups is important for nano-adsorbents in controlling their surface activity. The anchor groups provide affinity with the target substances via coordination, electrostatics, hydrogen bonding, chemical bonding and van der Waals force, which enhance the adsorption capacity as well as the adsorption selectivity [9,22,23]. Oleic acid, an unsaturated fatty acid with active –COOH group, has been used in the surface modification of SiO_2, ZnO, Fe_3O_4, Al_2O_3 and TiO_2 [24,25]. Furthermore, oleic acid behaves well in the bio-molecule immobilization, for example, the oleic acid bound with α-lactalbumin (α-LA) and formed HAMLET (human α-lactalbuminmadelethal to tumor cells)-like complexes, which exhibits highly selective anti-tumor activity both in vitro and in vivo[26,27]. Using oleic acid in the surface functionalization of TiO_2 may enhance the interface interaction between TiO_2 and the proteins with $–NH_2$ side chains, which has not been reported yet to our knowledge.

Fixing the nano-adsorbents on a larger support especially on a porous carrier is a good alternative method to overcome their some disadvantages, such as easy to agglomerate and difficult to recovery from solution, which limited its practical applications. Poly(vinylidenedifluoride) (PVDF) films have been successfully applied in water treatment, drug release, gel electrolytes and fuel cells due to its good biocompatibility, chemical and thermal resistance[28-31]. Zhou *et al*. [28] studied the static adsorption of BSA on PVDF microfiltration membrane; the results showed a minor adsorption capacity. In order to control the adhesion of bio-molecules and improve surface activity, the hybridization and functionalization of PVDF membrane are essential. Though there are reports about inorganic nanoparticles hybrid PVDF membranes, however, most of which were focused on decreasing membrane adsorption for protein and broadening its application in water treatment [32-35], and few studies concentrated on the adsorption and separation of bio-molecules.

Here, a PVDF hybrid membrane entrapped with OA-modified TiO_2 was fabricated. First, OA-modified TiO_2 nanoparticles were synthesized, then, the OA-TiO_2 nanoparticles were blended with PVDF casting solution and the hybrid membranes were fabricated via an induced phase inversion process. Two homologous proteins: bovine serum albumin (BSA) and bovine hemoglobin (BHb) were chosen as the target proteins to investigate the adsorption properties of hybrid membranes. The influences of various parameters including contact times, pH conditions and the additional amount of TiO_2 were conducted. Based on the experimental results, an optimum selective adsorption condition for BHb was determined.

Experimental

Chemicals and Membranes

Bovine serum albumin (BSA, MW 66 KDa, pI 4.5) of biotechnology grade was purchased from Roche Ltd. (Switzerland). Bovine hemoglobin (BHb, MW 64.5 KDa, pI 6.8) of biotechnology grade was obtained from Amresco Ltd. (USA). Poly(vinylidenefluoride) (PVDF) powder was purchased from Mosu Science Equipment Corporation (Shanghai, China). Polyvinyl pyrrolidone, dimethyl formamide, oleic acid (OA) and tetrabutyltitanate were obtained from Sinopharm Chemical Reagent Corporation (Shanghai, China). All the chemicals except BSA and BHb were of analytic grade and used without further purification, and 18 MΩ/cm deionized water was used throughout the experiment.

Synthesis and characterization of PVDF/ (OA)TiO_2 hybrid membranes

OA-modified TiO_2 nanoparticles with anatase structure were synthesized according to our previous work [36]. Briefly, 20 mL of tetrabutyltitanate and 1.1 mL of OA were dissolved in 200 mL of ethyl alcohol, then this solution was added into 200 mL of deionized water (pH=3.0, adjusted by 0.1mol/L HNO_3) at 70˚C. The obtained white gel was maintained at 70˚C for 48 h. After that, the white precipitation was centrifuged, washed and dried at 80˚C for 24 h. The pure TiO_2 nanoparticles were prepared under same conditions but without OA addition.

The PVDF/(OA)TiO_2 hybrid films were fabricated via an induced phase inversion process. In a typical experiment, a certain quantity of as-prepared (OA)TiO_2 nanoparticles were fully dispersed in 100 mL of DMF solution containing 14 wt% PVDF and 2 wt% PVP. Then, the mixed suspension was cast onto glass plates using a dip coater device. After that, the glass plates were immersed into a coagulation water bath. Finally, the hybrid films were formed, washed and stored in distilled water. The synthesized hybrid membranes were signed as PVDF/(OA)TiO_2(*x*%), the *x* values indicated the addition amounts of OA-TiO_2 nanoparticles, which

were varied from 2.0 wt% to 8.0 wt%. For comparison, the PVDF/TiO_2(2%) hybrid membrane was also prepared by above method but using pure TiO_2 as additives.

The surface morphology of the membranes was observed on a SSX-50 scanning electron microscope (SEM, Shimadzu, Japan). X-ray diffraction pattern was taken on a Rigaku XRD D/max-2500PC instrument (CuKα, tube voltage of 50 KV and tube current of 100 mA). Thermo-gravimetric curves were taken on a TA instrument (TGA/DSC/1600LF, Mettler Toledo, Switzerland), the sample was heated to above 800 °C under nitrogen with heating rates of 10 °C/min. The water contact angle tests were taken on a Contact Angle Measuring Device (TL100, Finland).

Protein adsorption and desorption experiments

Different membrane samples were cut into small pieces (8 cm^2) and introduced in a small beaker containing 8 mL of protein solution with desired initial concentrations, pH values, followed by shaking on a vortex suspension device for predetermined time. Then, the films were removed at regular intervals and the protein concentrations were determined with UV-Vis spectrophotometer (Lambda 35, PerkinElmer, USA). The characteristic absorption for BHb was at 405 nm, and which for BSA was at 595 nm with coomassie brilliant blue technique. The adsorbed amounts (q_e, μg/cm^2) of proteins were calculated according to Eq. (1):

$$Q_e = \frac{(c_0 - c_e) \times V}{S} \quad (1)$$

Wherec_0(μg/mL) is the initial concentration of protein; c_e (μg/mL) is the concentration in solution at the balance; V (mL) is the volume of solution, and S (cm^2) is the area of the film.

Desorption experiments were conducted by mixing the adsorbed hybrid membranes with 8 mL of Na_3PO_4 (0.08 mol/L), SDS (5 mg/L), Tris-HCl (pH=7 and 8.8), Na_2CO_3-$NaHCO_3$ (pH=9.0) and citric acid-sodium citrate (pH=5.0) respectively. The mixed solution was shaken on a vortex suspension device for 60 min. After that, the remaining solution was analyzed to determine the protein concentration (c_2). The desorption percent (*Des*, %) was calculated by using Eq. (2) :

$$Des\% = \frac{c_2}{(c_0 - c_e)} \times 100\% \quad (2)$$

Adsorption selectivity assessment

A binary mixed solution of BHb and BSA (concentration ratio of BHb to BSA was 1:1 and 2:1 respectively) was applied to assess the selective adsorption activity of hybrid membranes. The adsorption experiment was conducted under the optimum conditions for BHb, and the contents of BHb and BSA in supernatant solution and elution solution were estimated through sodium dodecyl sulfate polyacrylamide gel electrophoresis (SDS-PAGE) analysis[37].

Dynamic adsorption performances

The dynamic adsorption performances of the PVDF/(OA)TiO_2 hybrid membrane were measured using a nitrogen pressurized stirred dead-end filtration cell (Mosu, Shanghai, China) at a trans membrane pressure of 0.15 bar. 5 sheets of membranes with effective filtration diameter of 3.5 cm were stacked to avoid limited adsorption amount of a single membrane. A binary mixed solution of BHb and BSA (c_0=150 μg/ml) in 36 mL at pH 6.0 was permeated through the stack of membranes at a constant flow rate of 34.5 L/(h m^2). The permeates were collected and the BHb and BSA concentration in the permeate solution was determined using UV-Vis spectrophotometer(Lambda 35, PerkinElmer, USA).

Results and discussion

Characterization of PVDF/(OA)TiO_2 hybrid membranes

The XRD patterns of OA-TiO_2 and PVDF/(OA)TiO_2 hybrid membranes were shown in Fig. 1(a). In the case of OA-TiO_2, all the peaks were consistent with the standard data of anatase TiO_2 (PDF card No. 21-1272), except one weak peak belonged to brookite TiO_2 (PDF card No. 29-1360). According to Scherrer's formula: $D = \frac{K\lambda}{\beta \cos\theta}$ (K=0.89, λ=1.5405 nm), based on the data of (101) plane, the crystalline size of TiO_2 was calculated to be 6 nm. For the PVDF/(OA)TiO_2 hybrid membranes, besides the characteristic diffraction of anatase TiO_2, there were three discernable diffraction peaks appeared at 2θ=18.67°, 19.48° and 25.58° in reference to the diffraction in planes (020), (110) and (021) of α-phase PVDF films [38].

TEM investigation of the OA-modified TiO_2 particles was presented in Fig. 1(b), the morphology of TiO_2 was almost ellipsoidal and the average length ranged from 10 to 50 nm. It was reported that the OA molecule tends to adsorb on the (001) and (100) faces of TiO_2, and which resulted in the formation of non-spherical particles[39].

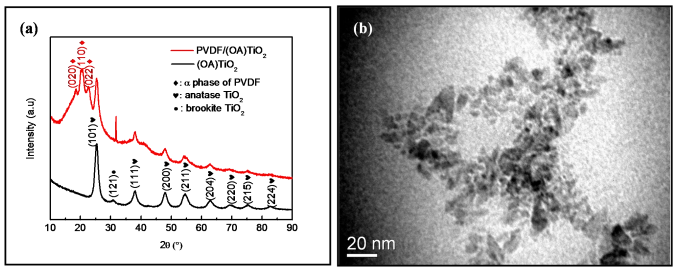

Fig. 1(a) XRD patterns of OA-modified TiO_2 and PVDF/(OA)TiO_2 hybrid membranes; (b) TEM image of OA-modified TiO_2 nanoparticles

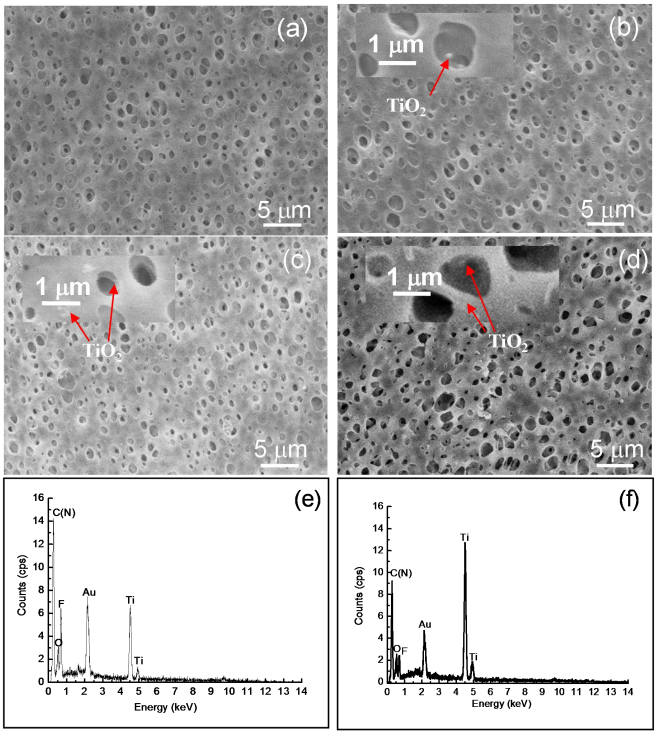

Fig. 2 (a) SEM images of PVDF; (b-d) SEM image of PVDF/(OA)TiO_2 hybrid membranes with different TiO_2 additions: (b) $w(TiO_2)$=2%; (c) $w(TiO_2)$=6%; (d) $w(TiO_2)$=8%. The inset pictures were with higher magnification; (e, f) EDX spectrum of PVDF/(OA)TiO_2 hybrid membranes with different TiO_2 additions: (e) $w(TiO_2)$=2%; (f) $w(TiO_2)$=6%.

SEM observation of the pristine PVDF and the prepared PVDF/(OA)TiO_2 hybrid membranes with different TiO_2 addition was shown in Fig. 2. As shown in Fig. 2(a), the PVDF films were with porous structure, and the average pore size was 1250 nm. After TiO_2 addition, as shown in Fig. 2(b)-(d), a lot of tiny TiO_2 nanoparticles were deposited in the pores and on the surface of PVDF. Meanwhile, the pore size of PVDF changed, the average pore size was 937 nm, 625 nm and 1250 nm as TiO_2 addition increased from 2 wt% to 8 wt%, respectively.

The existence of TiO_2 can affect the formation process of PVDF [36,38,40]. In the presence of TiO_2, TiO_2 nanoparticles acted as crysta nuclei and heterogeneous nucleation was occurred instead o homogeneous nucleation. With the increase of TiO_2 addition, mo nuclei were formed and the diameter of PVDF decreased. However, when the TiO_2 dosage exceeded a certain amount (6.0 wt% in thi work), TiO_2 aggregated in the polymer matrix and the crystal nucle was decreased. Therefore, the surface roughness of PVDF increased and the pore sizes was enlarged. The similar effects were reporte by Shi *et al* in the formation of PVDF/TiO_2 composite membranes[38].

Fig. 2 (e) and (f) present the EDX spectrum of hybrid membranes with TiO_2 addition was 2 wt% and 6 wt%, it could be seen that the relative intensity of Ti element evidently enhanced with increased TiO_2 addition. The TG analysis was used to determine the TiO_2 contents of hybrid membranes, and the calculated results we shown in Table1. The loading amounts of TiO_2 were 8.2, 15.6, 19.3 and 23.3 wt% when the TiO_2 additions were 2, 4, 6 and 8wt% respectively. The TiO_2 contents from TG tests were less than th theoretical loading mass, which might be caused by the incomplete loading of TiO_2 in the fabrication of hybrid membranes.

The membrane surface hydrophilicity or hydrophobility can be evaluated by the water contact angle data, in general speaking, the smaller contact angle indicates the higher hydrophilicity. Table 1 also presented the water contact angle of different PVDF/(OA)TiO_2 hybrid membranes. With increasing the dosage of TiO_2 nanoparticles, the contact angle of hybrid membranes decreased slightly, that implied the presence of TiO_2 nanoparticles enhanced the surface hydrophilicity of PVDF membranes.

Table1 The loading contents of TiO_2 and the contact angle tests of hybrid membranes

	Pristine PVDF	PVDF/ (OA)TiO_2 (2%)	PVDF/ (OA)TiO_2 (4%)	PVDF/ (OA)TiO_2 (6%)	PVDF/ (OA)TiO_2 (8%)
TiO_2 content (wt%)	0	8.2	15.6	19.3	23.3
Contact angle (°)	80	77	72	65	69

Effect of OA-modification on the membrane adsorption activity

In the fabrication of hybrid membranes, the OA molecule was used to modify the surface of TiO_2. To explore the effect of OA

modification on the adsorption properties of hybrid membranes, the pure TiO_2 hybrid PVDF membranes were also prepared under same conditions, and both hybrid membranes were applied in the adsorption of BSA and BHb and the results were shown in Fig. 3. As shown in Fig.3(a), for the BHb adsorption, the maximum adsorption capacity on PVDF/(OA)TiO_2 appeared at pH value was 6.0, however, which for PVDF/TiO_2 was at pH 7.0. Furthermore, the BHb adsorption on PVDF/(OA)TiO_2 membranes was enhanced in comparison with that on PVDF/TiO_2 under most pH conditions, which indicated that the OA-modification was beneficial for the BHb adsorption on the hybrid membranes. Interestingly, the BSA adsorption on hybrid membranes was depressed after the OA-modification. As shown in Fig. 3(b), the adsorption capacity of BSA on PVDF/TiO_2 was larger than that on PVDF/(OA)TiO_2 under most pH values, and the maximum adsorption achieved at pH 4.0 for PVDF/(OA)TiO_2 and pH 5.0 for PVDF/TiO_2.

From Fig. 3, it could be concluded that the OA-modification had opposite effect on the BHb and BSA adsorption, and the maximum adsorption capacity of BHb was nearly as 4 times as that of BSA, which provided an opportunity of selective separation of two proteins.

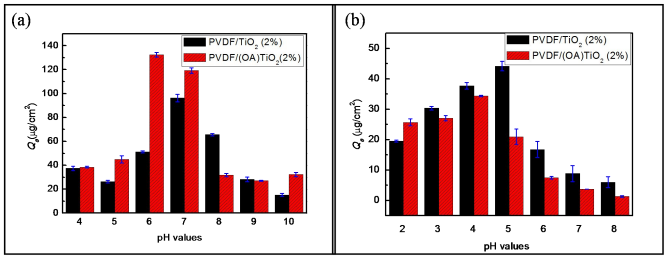

Fig. 3 (a) BHb adsorption on PVDF/TiO_2 and PVDF/(OA)TiO_2; (b) BSA adsorption on PVDF/TiO_2 and PVDF/(OA)TiO_2. (c_0 (BHb)=150 mg/L, c_0 (BSA)=150 mg/L, t=70 min)

The opposite effect of OA-modification might be caused by the change of surface physico-chemical property of TiO_2. In our previous work [41], it was found that the long hydrophobic chain and hydrophobic nature of OA molecules provided a hydrophobic interface for the modified TiO_2, which transformed the surface property of TiO_2 from super-hydrophilic to much more hydrophobic. It was reported that BHb molecule has a stronger affinity for hydrophobic surfaces than the BSA molecule has, and BSA molecule was more likely adsorbed on a hydrophilic surface [42,43]. Therefore, the enhanced hydrophobic property bring by OA-modification could be responsible for the enhanced BHb adsorption while depressed BSA adsorption.

To further explore the adsorption behavior of two proteins on PVDF/(OA)TiO_2, different adsorption conditions were applied and the optimum conditions were determined.

Adsorption behavior of BSA and BHb on PVDF/(OA)TiO_2 hybrid membranes

Fig.4(a) presented the kinetic curves of proteins adsorption capacity versus the contact time using PVDF/(OA)TiO_2 (2 wt%) hybrid membranes as adsorbents. A rapid adsorption rate could be observed during the first 50 min for both proteins, and then the adsorption reached equilibrium within 70-90 min. So, the time of 70 min was selected in the following experiments.

The adsorption isotherm of BSA and BHb on PVDF/(OA)TiO_2 (2 wt%) hybrid membranes was shown in Fig. 4(b). It was observed that the adsorption capacity of BSA and BHb enhanced when the protein concentration increased from 12 to 150 μg/mL, and reached its maximum at the protein concentration was 150 μg/mL and then kept constant with increasing protein concentration. The maximum adsorption capacity of BHb was 128.8 μg/cm^2, while that of BSA was 34.24 μg/cm^2.

The adsorption capacities of BHb and BSA with different ionic strength were shown in Fig. 4(c). Generally speaking, the variation of NaCl concentration would not make significant impact on the BHb adsorption, as shown in Fig. 4(c). The adsorption capacity of BHb increased a little as the concentration of NaCl increased to 0.15mol/L, and continuously increasing the concentration of NaCl, the adsorption capacity of BHb decreased slightly. As for BSA adsorption, the adsorption amount of BSA increased evidently when the concentration of NaCl increased till when it came to 0.2 mol/L, and then decreased slightly.

The presence of dissolved salt ions could affect protein adsorption behavior on solid adsorbents [44,45]. Firstly, the salt counter ions competed against the protein molecule for binding sites. Secondly, the salt coexisting ions shielded the protein molecule and charged binding sites from each other. Thirdly, the change of ionic strength changed the folding and configuration of protein molecule [46]. All of them might result in the variation of hydrophobic interaction between the protein and the material. Accordingly, the enhancement of adsorption capacity of BHb and BSA with increasing ionic strength implied that the main interaction between hybrid membranes and proteins might be hydrophobic interaction instead of electrostatic interaction. The similar

phenomenon was also observed by Sean C. Smith *et. al*. in the lysozyme adsorption on the single-walled carbon nanotube[46].

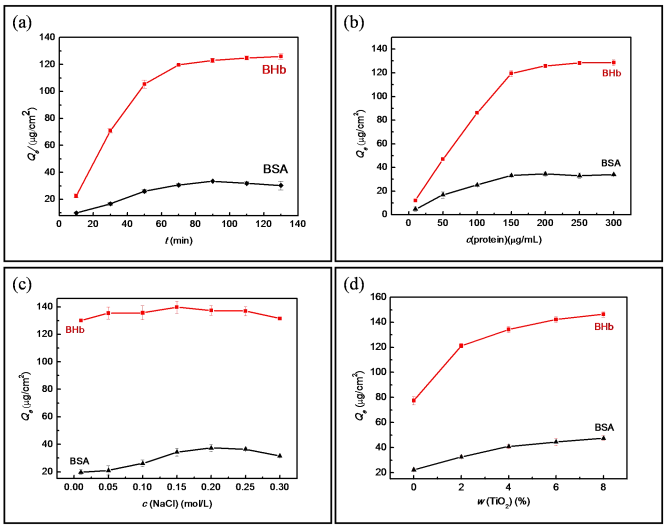

Fig. 4 (a) Adsorption kinetics of BHb and BSA on the PVDF/(OA)TiO_2 (2 wt%) hybrid membranes; (b) Adsorption isotherm of BHb and BSA on the PVDF/(OA)TiO_2 (2 wt%) hybrid membranes; (c) Effects of ionic strength on the adsorption capacity of BHb and BSA on the PVDF/(OA)TiO_2 (2 wt%) hybrid membranes; (d) Effects of addition amount of TiO_2 on the BHb adsorption and BSA adsorption.

Fig. 4(d) presented the adsorption capacity of proteins on the hybrid membranes with different OA-TiO_2 additions. It was observed that the TiO_2 loading significantly enhanced the adsorption activity of PVDF films. For the pristine PVDF, the adsorption amounts of BHb and BSA were 76.89 and 21.84 μg/cm^2 in sequence. After TiO_2 hybridization, the adsorption capacity of BHb and BSA increased with increasing TiO_2 loading amount, which demonstrated a positive relationship of TiO_2 addition and protein adsorption. For example, the adsorption capacities of BHb were 120.83, 134.47, 142.04 and 145.58 μg/cm^2, and that of BSA were 32.95, 41.55, 44.07 and 47.09 μg/cm^2 as the TiO_2 amount increased from 2% to 8%, respectively.

Adsorption processes are controlled by various mechanisms, such as mass transfer, mass diffusion, chemical reactions and intraparticle diffusion. In order to further explore the adsorption mechanism of BHb and BSA on the PVDF/(OA)TiO_2 hybrid membranes, the pseudo-first-order and pseudo-second-order kinetics models were used to simulate the adsorption kinetics data. The Lagergren first-order equation is mostly used in the initial adsorption process, and the Mckay second-order equation can be representative of the chemical adsorption process[47].The formula was shown as Eq. (3) and Eq. (4) :

$$Q_t = q_e(1-e^{-k_1 t}) \quad (3)$$

$$Q_t = \frac{k_2 q_e^2 t}{1+tk_2 q_e} \quad (4)$$

Where Q_t is the adsorption amounts at time t, q_e is the maximum adsorption capacity of proteins; k_1 and k_2 are the rate constants for the pseudo-first-order and pseudo-second-order kinetics respectively. The simulating curves and calculated parameters were shown in Fig. 5. In the case of BHb, the higher R^2 values (>0.99) and the closeness of theoretical values (q_e) with the experimental data confirmed the applicability of pseudo-first-order kinetic model rather than pseudo-second-order model. For the BSA adsorption (Fig. 5b), the better simulating results were also obtained by using pseudo-first-order kinetic model. Taking into account the impact of ionic strength, a hydrophobic interaction instead of electrostatic force between protein, OA-modified TiO_2 play important role in these adsorption process [48].

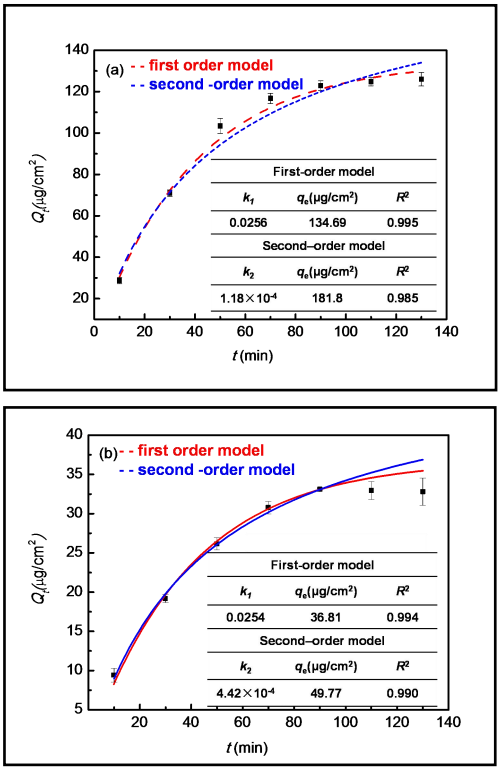

Fig. 5 Fitting curves of protein adsorption kinetics by pseudo-first-order and pseudo-second-order kinetic model. (a) BHb adsorption, (b) BSA adsorption

Langmuir and Freundlich models were also used to evaluate the isotherm data. The Langmuir model was suitable for monolayer adsorption, while Freundlich model was often used to explain the adsorptions on heterogeneous surface. The two formulas were expressed as follows:

Langmuir: $$Q_e = \frac{K_L \times q_m \times c_e}{1 + K_L \times c_e} \quad (5)$$

Freundlich: $$Q_e = K_F \times c_e^{1/n} \quad (6)$$

Where Q_e is the adsorbed protein amounts at the balance; q_m is the maximum adsorption capacity; c_e is the protein concentration in solution at the balance; K_L, K_F and n are the parameters reflecting the adsorption capacity and the adsorption intensity. As shown in Fig.6 (a) and (b), the adsorption isotherms of BHb and BSA both showed better simulating results with the Langmuir model rather than the Freundlich model, which determined a monolayer adsorption process of BHb or BSA on PVDF/TiO_2 hybrid membranes. The calculated maximum adsorption capacities of BHb and BSA on the hybrid membranes were 136.01 and 43.7 μg/cm^2 respectively.

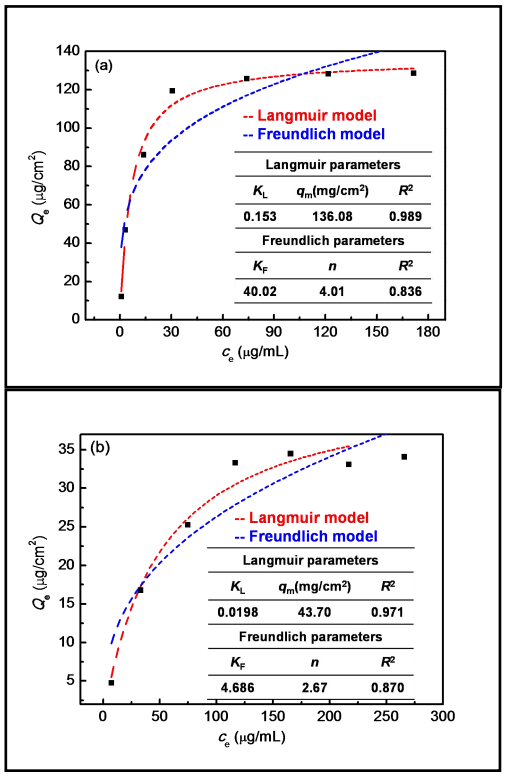

Fig. 6 Fitting curves by Langmuir and Freundlich models. (a) BHb adsorption; (b) BSA adsorption.

Considering the physical interaction existed between hybrid membranes and proteins, some electrolytes, such as Na_3PO_4 (0.08 mol/L), SDS (5 mg/L), Tris-HCl (pH=7 and 8.8), Na_2CO_3-$NaHCO_3$ (pH=9.0) and citric acid-sodium citrate (pH=5.0) were chosen to elude the adsorbed BHb, and the results were shown in Fig. 7. It could be seen that the elution efficiency followed an order as: SDS (5 mg/L)>Tris-HCl (pH=8.8)> Na_3PO_4(0.08 mol/L)>Na_2CO_3-$NaHCO_3$ (pH=9.0)>Tris-HCl (pH=7)>citric acid-sodium citrate (pH=5.0).

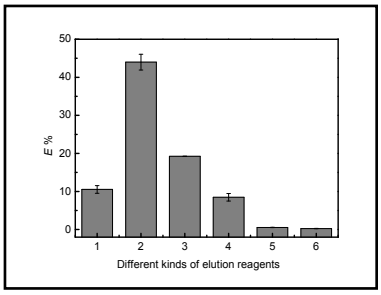

Fig. 7 The elution percents of adsorbed BHb with different kinds of eluants. (1) Na_3PO_4 (0.08 mol/L); (2) SDS (5 mg/L); (3) Tirs-HCl (pH=8.8); (4) Na_2CO_3-$NaHCO_3$ (pH=9.0); (5) Tirs-HCl (pH=7.0); (6) citric acid-sodium citrate (pH=5.0)

Selective adsorption of BHb using SDS-PAGE analysis

The different adsorption activity toward BHb and BSA implied that the selective separation of BHb from the binary protein mixture using the PVDF/TiO_2 hybrid membranes as adsorbent was feasible. In order to demonstrate it, binary proteins mixture of BHb and BSA were applied in the adsorption experiment and the sodium dodecyl sulfate polyacrylamide gel electrophoresis (SDS-PAGE) were used to investigate the adsorption selectivity; the results were shown in Fig. 8. It could be seen that there were two bans (lane 2) in the supernatant solution, which were attributed to the un-adsorbed BSA and BHb. However, only the BHb band could be seen in the elution (lane 3), which demonstrated that only the BHb was adsorbed on PVDF/(OA)TiO_2 hybrid membranes. Even if increasing the BHb initial concentration (Fig. 8b), only the BHb band could be seen in the elution (lane 3). The above results suggested that this kind of organic-inorganic hybrid membranes showed good selective adsorption activity toward BHb via surface modification, which might be used as an adsorbent material in the separation of proteins.

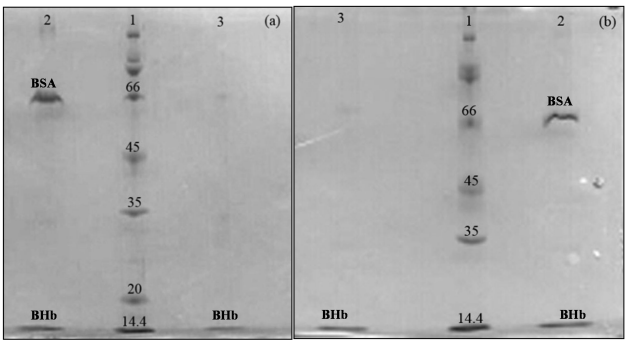

Fig. 8 SDS-PAGE pattern of adsorption on PVDF/(OA)TiO_2 (2 wt%) composite membranes using BHb-BSA mixed solution with different initial concentration. (a): c_0(BHb)=c_0(BSA)=150 μg/ml; (b) c_0(BHb)=300 μg/ml, c_0(BSA)=150 μg/ml. Lane 1, protein molecular weight marker; lane 2, supernatant solution; lane 3, the eluted solution.

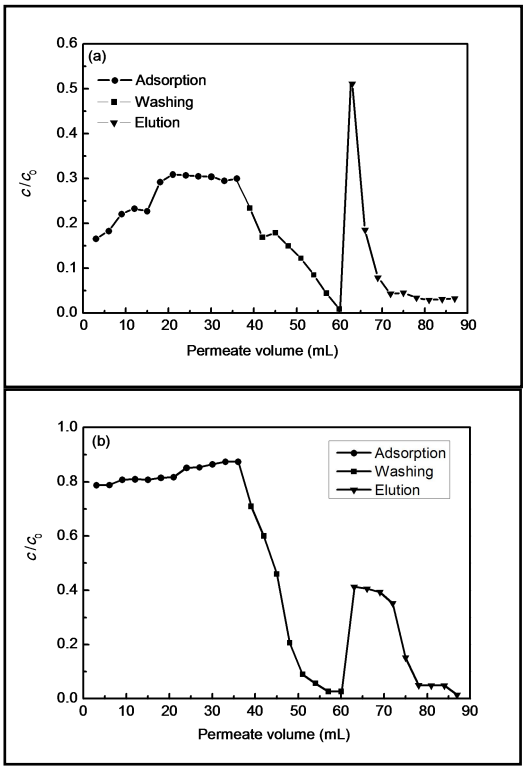

Fig. 9 Typical breakthrough and elution curves for a module of 5 mixed matrix PVDF/(OA)TiO_2 (2 wt%) composite membranes: (a) for BHb; (b) for BSA

Dynamic selective adsorption measurement

The typical breakthrough and elution curves were measured using a binary protein solution as the adsorption object and 5 mg/L SDS as eluant, which were shown in Fig. 9. For the BHb adsorption (Fig. 9a), at initial stage, the value of c/c_0 was about 0.165, which indicated that about 83.5 % BHb could be adsorbed. As flow time prolonged, the value of c/c_0 increased and kept at 0.30. Using 5 mg/L SDS as eluant, about 51.5 % BHb could be recovered. The dynamic BHb adsorption capacity per unit of membrane area was 78.57 μg/cm^2, which was calculated by numerical integration until the breakthrough point 30% of the protein feed concentration. This dynamic adsorption amount was 1.69 times smaller than the maximum static adsorption capacity using a single BHb as target. It was reported that the dynamic adsorption is 5-10 times lower than the static binding capacity; which may be coursed by a non-uniform flow distribution and resistance against mass transport rate process and a full adsorption capacity can be obtained only if the flow rate is slow enough so that the adsorbent substance can diffuse to the adsorption site and can rearrange their structure to its favorable one before the interstitial volume continues through the membrane [6,49].

Fig. 9(b) present the dynamic adsorption curves for BSA, the value of c/c_0 at initial stage was 0.787, which indicated only 21.3% BSA was adsorbed. With flow time the value of c/c_0 increased and kept at 0.880. SDS (5 mg/L) could recovered 41.8 % BSA. The dynamic adsorption capacity of BSA per unit of membrane area was 13.47 μg/cm^2, which was only 17.1 % of the value of BHb.

Conclusions

The PVDF hybrid membranes entrapped with OA-modified TiO_2 nanoparticles were prepared via phase induced method. The TiO_2 nanoparticles in size about 10-50 nm were deposited in the pores and on the surface of PVDF, and the pore size of PVDF were varied with different TiO_2 additions. In the adsorption experiments, the hybrid membranes showed better adsorption activity toward BHb rather than BSA, and the maximum adsorption capacities of BHb and BSA were 145.58 and 47.09 μg/cm^2 respectively, as the TiO_2 loading amount was 8 wt%. The optimum adsorption conditions for BHb were as follows: pH=6.0, t=70 min, c(NaCl)=0.15mol/L, c_0(BHb)=150 μg/mL, and SDS (5 mg/L) could elute adsorbed BHb from hybrid membranes. The SDS-PAGE analysis showed that there was only BHb could be found in the elution solution, which demonstrated the selective adsorption of BHb on the PVDF/(OA)TiO_2 hybrid membrane. The dynamic capacity experiments showed a little decreased adsorption capacity of BHb when the binary proteins mixture flowed through a stack of 5 sheets of hybrid membranes.

Acknowledgements

The authors are very grateful for the financial support of National Natural Science Foundation of China (No. 21103017, 51104042).

Notes and references

1. R. Huang, A.R. Ferhan, L.H. Guo, B. Qiu, Z.Y. Lin, D.H. Kim, G.N. Chen, *RSC Adv*,2014, **4**, 4883-4888.
2. X.W. Wang, G.M. Liu, G.Z. Zhang, *Langmuir*,2012, **28**, 14642-14653.
3. Q. Wu, R. Wang, X.N. Chen, R. Ghosh, *J Membr Sci*,2014, **471**, 56-64.
4. M.S.L. Tijink, M. Wester, G. Glorieux, K.G.F. Gerritsen, J.F. Sun, P.C. S.Z. Borneman, M. Wessling, R. Vanholder, J.A. Joles, D. Stamatialis, *Biomater*,2013, **34**, 7819-7828.
5. T. Kopac, K. Bozgeyik, J. Yener, *Colloid Surface A*,2008, **322**, 19-28.
6. M.E. Avramescu, M. Gironès, Z. Borneman, M. Wessling, *J Membr Sci*,2003, **218**, 219-233.
7. T.T. Xia, Y.P. Guan, M.Z. Yang, W.B. Xiong, N. Wang, S. Zhao, C. Guo, *Colloid Surface A*,2014, **443**, 552-559.
8. P. Parhi, A. Golas, N. Barnthip, H. Noh, E.A. Vogler, *Biomater*,2009, **30**, 6814-6824.
9. F. Meder, C. Brandes, L. Treccani, K. Rezwan, *Acta Biomater*,2013, **9**, 5780-5787.
10. O. Svensson, T. Arnebrant, *J Colloid Interf Sci*,2010, **344**, 44-47.
11. Z.G. Peng, K. Hidajat, M.S. Uddin, *J Colloid Interf Sci*,2004, **271**, 277-283.
12. H. Wei, W.S. Yang, Q. Xi, X. Chen, *Mater Lett*,2012, **82**, 224-226.
13. L.E. Valenti, P.A. Fiorito, C.D. García, C.E. Giacomelli, *J Colloid Interf Sci*,2007, **307**, 349-356.
14. D. Vu, Z.Y. Li, H.N. Zhang, W. Wang, Z.J. Wang, X.R. Xu, B. Dong, C. Wang, *J Colloid Interf Sci*,2012, **367**, 429-435.
15. Y.G. Tao, L.B. Ye, J. Pan, Y.M. Wang, B. Tang, *J Hazard Mater*,2009, **161**, 718-722.
16. W. Liu, J.R. Ni, X.C. Yin, *Water Res*,2014, **53**, 12-25
17. B.L. Dou, V. Dupont, W.G. Pan, B.B. Chen, *Chem Eng J*,2011, **166**, 631-638.
18. J.Q. Fu, X. Zhang, S.H. Qian, L. Zhang, *Talanta*,2012, **94**, 167-171.
19. M.H. Ahmed, T.E. Keyes, J.A. Byrne, C.W. Blackledge, J.W. Hamilton, *J Photoch Photobio A*,2011, **222**, 123-131.
20. J.L. Wehmeyer, R. Synowicki, R. Bizios, C.D. García, *Mater Sci Eng C*, 2010, **30**, 277-282.
21. C.E. Giacomelli, M.J. Avena, C.P. D.Pauli, *J Colloid Interface Sci*,1997, **188**, 387-395.
22. J. Kujawa, S. Cerneaux, W. Kujawski, *Colloid Surface A*,2014, **447**, 14-22.
23. K. Vasilev, Z. Poh, K. Kant, J. Chan, A. Michelmore, D. Losic, *Biomater*,2010, **31**, 532-540.
24. S. Kango, S. Kalia, A. Celli, J. Njuguna, Y. Habibi, R. Kumar, *Prog Polym Sci*,2013, **38**, 1232–1261.
25. Y.J. Cui, X. Chen, Y.F. Li, X. Liu, *Appl Microbiol Biot*,2012, **95**, 147–156.
26. B. Fang, M. Zhang, M. Tian, L. Jiang, H.Y. Guo, F.Z. Ren, *BBA-Mol Cell Biol L*,2014, **1841**, 535–543.
27. F.Y. Jr, M. Zhang, J. Chen, Y. Liang, *BBA-proteins proteom*,2006, **1764**, 1389–1396.
28. Y.N. Zhou, Z. Wang, Q. Zhang, X.J. Xi, J. Zhang, W.T. Yang, *Desalination*,2012, **307**, 61–67.
29. L.S. Wu, J.F. Sun, F.Q. Tong, *RSC Adv*,2014, **4**, 63989-63996.
30. Y.X. Shen, P.O. Saboe, I.T. Sines, M. Erbakan, M. Kumar, *J Membr Sci*,2014, **454**, 359-381.
31. J. Yuan, J.Q. Meng, Y.L. Kang, Q.Y. Du, Y.F. Zhang, *Appl Surf Sci*,2012, **258**, 2856–2863.
32. Q.Y. Wang, Z.W. Wang, J. Zhang, J. Wang, Z.C. Wu, RSC Adv, 2014, **4**, 43590-43598.
33. F.M. Shi, Y.X. Ma, J. Ma, P.P. Wang, W.X. Sun, *J Membr Sci*,2013, **427**, 259-269.
34. X. Zhang, Y. Wang, Y.F. Liu, J.L. Xu, Y.D. Han, X.X. Xu, *Appl Surf Sci*,2014, **316**, 333–340.
35. T.F. Wu, B.M. Zhou, T. Zhu, J. Shi, Z.W.Xu, C.S. Hu, J.J. Wang, RSC Adv,2015, **5**, 7880-7889.
36. X. Zhang, Y. Wang, Y.T. You, H. Meng, J.H. Zhang, X.X. Xu, *Appl Surf Sci*,2012, **263**, 660-665.
37. Q. Li, Q.Y. Bi, H.H. Lin, L.X. Bian, X.L. Wang, *J Membr Sci*,2013, **427**, 155-167.
38. F.M. Shi, Y.X. Ma, J. Ma, P.P. Wang, W.X. Sun, *J Membrane Sci*,2012, **389**, 522-531.
39. J. Wen, J. Li, S.J. Liu, Q.Y. Chen, *Colloid Surface A*,2011, **373**, 29-35.
40. M. Gu, J. Zhang, X. Wang, H. Tao, L. Ge, *Desalination*,2006, **192**, 160-167.
41. S.G. Guo, J.H. Zhang, M.X. Shao, X Zhang, Y.F. Liu, J.L. Xu, H. Meng, Y.D. Han, *Mater Res Express*,2015, **2**, 045101.
42. H. Shirahama, K. Suzuki, T. Suzawa, *J Colloid Interface Sci*, 1989, **129**, 483-490.
43. Carl D. Walkey, Warren C.W. Chan, *Chem Soc Rev*,2012, **41**, 2780-2799.
44. M. Rade, D. Verdes, S. Seeger, *Adv Colloid Interface Sci*,2011, **162**, 87-106.
45. Z. Adamczyk, *Curr Opin Colloid Interface Sci*,2012, **17**, 173–186.
46. S.C. Smith, F. Ahmed, K.M. Gutierrez, D.F. Rodrigues, *Chem Eng J*,2014, **240**, 147–154.
47. W. Ma, T.F. Lv, X.N. Song, Z.H. Cheng, S.B. Duan, G. Xin, F.J. Liu, D.C. Pan, *J Hazard Mater*,2014, **268**, 166–176.
48. T.S. Anirudhan, S.R. Rejeena, A.R. Tharun, *Colloid Surface B*,2012, **93**,49–58.
49. M.E. Avramescu, Z. Borneman, M. Wessling, *J Chromatog A*,2003, **1006**, 171–183.